Diagnostic Accuracy Study

Medicine®

OPEN

Positron emission tomography/computed tomography dual imaging using 18-fluorine flurodeoxyglucose and ^{11}C-labeled 2-β-carbomethoxy-3-β-(4-fluorophenyl) tropane for the severity assessment of Parkinson disease

Xiaohong Li, MD, Qizhou Zhang, MD, Yongde Qin, PhD*, Yubin Li, MD, Nazimuguli Mutaerbieke, MD, Xiaojia Zhao, MD, Amina Yibulayin, MD

Abstract

The value of dual imaging mode for the severity assessment of Parkinson disease (PD) is explored by conducting positron emission tomography computed tomography (PET/CT) double imaging using combined 18-fluorine flurodeoxyglucose (^{18}F-FDG) brain metabolism and 11C-2β-carbomethoxy-3β-(4-fluorophenyl) tropane (^{11}C-CFT) brain dopamine transporter (DAT).

A total of 102 patients with PD and 50 healthy people in the control group are enrolled for the PET/CT dual imaging of ^{18}F-FDG brain metabolism and ^{11}C-CFT brain DAT. The characteristics of ^{18}F-FDG PET/CT and ^{11}C-CFT PET/CT imaging are analyzed by delineating the region of interest. Differences in the glucose metabolism and DAT distribution in the basal ganglia of patients with PD and healthy control group in the PET/CT imaging and the radioactive distribution characteristics of cerebral cortex in glucose metabolism imaging are compared. The characteristics of PET/CT imaging of ^{11}C-CFT brain DAT in the ganglion region in absorbing ^{11}C-CFT in different PD groups are analyzed.

Compared with the healthy control group, changes in the cerebral glucose metabolism in the PD group mainly occur due to the increased symmetry metabolism of the nucleus of bilateral basal ganglia and the decreased metabolism of the cerebral cortex as shown in the ^{18}F-FDG PET/CT images. With disease progression, the bilateral parietal, frontal, temporal, and occipital leaves showed different degrees of FDG metabolism. Statistically significant difference is observed for the^{11}C-CFT absorption among the caudate nucleus and the anterior, middle, and posterior nuclei of the bilateral basal ganglia of the PD and healthy control groups. In the PD group, the bilateral caudate nucleus and the anterior, middle, and posterior parts of the putamen show decreased DAT distribution. Regardless of unilateral or bilateral symptoms, the DAT distribution in the nucleus of the contralateral basal ganglia and in the posterior part of the nucleus is substantially reduced.

PET/CT dual imaging by ^{18}F-FDG PET/CT combined with ^{11}C-CFT PET/CT features high application value for the severity assessment of PD.

Abbreviations: ^{11}C-CFT = ^{11}C-labeled 2-β-carbomethoxy-3-β-(4-fluorophenyl) tropane, ^{18}F-FDG = 18-fluorine flurodeoxyglucose, MRI = magnetic resonance imaging, PD = Parkinson disease, PET/CT = positron emission tomography/computed tomography.

Keywords: brain metabolism, computed tomography of electron emission, dopamine transporter, Parkinson disease

Editor: Ismaheel Lawal.

The datasets generated during and/or analyzed during the current study are available from the corresponding author on reasonable request.

XL and QZ contributed equally to this work.

The authors have no conflicts of interest to disclose.

Department of Nuclear Medicine, The First Affiliated Hospital of Xinjiang Medical University, Urumqi, China.

** Correspondence: Yongde Qin, Department of Nuclear Medicine, The First Affiliated Hospital of Xinjiang Medical University, Urumqi, China (e-mail: qyd199013@163.com).*

How to cite this article: Li X, Zhang Q, Qin Y, Li Y, Mutaerbieke N, Zhao X, Yibulayin A. Positron emission tomography/computed tomography dual imaging using 18-fluorine flurodeoxyglucose and 11C-labeled 2-β-carbomethoxy-3-β-(4-fluorophenyl) tropane for the severity assessment of Parkinson disease. Medicine 2020;99:14 (e19662).

Received: 13 July 2019 / Received in final form: 6 February 2020 / Accepted: 20 February 2020

http://dx.doi.org/10.1097/MD.0000000000019662

1. Introduction

Parkinson disease (PD) is an "immovable" neurodegenerative disease affecting patients aged >60 years. Approximately 3 million middle-aged and elderly people in China suffer from PD. With the increasing aging population, the incidence of PD also increases annually. Given its unclear etiology, the future prevalence of PD is predicted to increase.[1] The clinical manifestations and pathology of PD overlap considerably with those of atypical Parkinsonism (APS). APS consists of multiple system atrophy (MSA), progressive supranuclear palsy (PSP), and corticobasal degeneration (CBD). PD is currently diagnosed by relevant clinical symptoms, signals, and curative effects caused by dopamine-producing medicine and other indicators. The severity of PD is evaluated according to the Hoehn–Yahr PD stage (HY stage). This method is valuable but is subjective and lacks certain objective indicators. Therefore, good biomarkers in diagnosing PD will provide an improved intervention window for treatment, which is a key issue for this disease.[2,3] Studies have shown that the misdiagnosis rate of PD reaches 20% to 25%. APS is often misdiagnosed as PD, especially at the early stage of the disease. Although the late-stage patients of APS present specific clinical signs, considerable proportions of MSA, PSP, and especially CBD patients (<74%) cannot be properly treated. A high misdiagnosis rate has affected the choice of treatment regimen and prognostic prediction of the disease.[4–6]

Along with the development and maturity of neuroimaging analysis methods, a growing number of imaging methods have been used in the diagnosis of PD. Blood oxygen level-dependent functional magnetic resonance imaging (BOLD-fMRI), utilizing changes in the blood oxygen level as the natural contrast medium, reflects the local activity of brain tissues on T2-weighted images. With its excellent sensitivity to brain physiology, BOLD-fMRI provides new valuable clues for the diagnosis and differential diagnosis of PD. However, quantitative indicators for determining the differences in the excitability found by BOLD-fMRI between the PD patients and normal subjects are lacking. The subjectiveness of physicians still plays a certain role in the assessment. Moreover, given their individual differences, the excitability of the cerebellar thalamic cortical and striatal–thalamic–cortical circuits is influenced by various external factors, resulting in the difficulty of PD diagnosis.[7]

PET/CT is the main method of molecular imaging, particularly for degenerative diseases of the nervous system.[8] This method aids in the diagnosis, differential diagnosis, and assessment of PD.[9] PET/CT has long been rated as a standard for measuring the integrity of dopaminergic nerve endings and assessing PD severity.[10] The pathological changes resulting from PD are closely related to glucose metabolism and dopamine transporter (DAT) changes.[10] 18-Fluorine flurodeoxyglucose (^{18}F-FDG) can be considered a powerful detector for the diagnosis of suspected patients with early-stage PD exhibiting clinical symptoms. DATs are specifically located in dopaminergic neurons. Experimental work in PD animal models revealed the relationship between striatal dopamine density, presynaptic DATs, and nigrostriatal cell loss. The ^{11}C-labeled 2-β-carbomethoxy-3-β-(4-fluorophenyl) tropane (^{11}C-CFT) is a cocaine derivative with a high affinity with DAT on the presynaptic membrane and reflects the function of dopaminergic neurons in the nigrostriatal pathway. ^{11}C-CFT is used as a specific PET tracer.

In the present study, ^{18}F-FDG and ^{11}C-CFT were respectively used for the PET/CT imaging of 102 patients with confirmed PD and 50 healthy subjects. The brain glucose metabolism and DAT PET imaging features of the PD patients were observed. On this basis, the application value of ^{18}F-FDG PET brain imaging combined with ^{11}C-CFT DAT PET imaging in severity evaluation of PD patients was determined.

2. Materials and methods

2.1. Research object

This was a prospective study approved by the Ethics Committee of First Affiliated Hospital of Xinjiang Medical University (20140418-01). A total of 102 patients diagnosed with PD at the First Affiliated Hospital of Xinjiang Medical University from June 2015 to April 2019 are included in the PD group (PD), including 38 males with an average age of 61.58 ± 11.03 years and 64 females with an average age of 61.18 ± 8.62 years. In addition, 50 healthy people with corresponding age are selected as healthy controls (HC), including 18 males with an average age of 60.94 ± 5.77 years and 32 females with an average age of 60.35 ± 8.41 years.

2.2. Inclusion criteria

All patients with PD and who meet the Hughes diagnostic criteria of the London Parkinson Association are recruited.[11–13] First, the reduced movements are characterized by the slowing down of autonomous free movement and the decreased speed and magnitude of repetitive motion. Second, at least 1 of the following characteristics exists:

(1) muscle stiffness,
(2) static tremor, and
(3) unstable posture.

Third, at least 3 of the following characteristics exist:

(1) unilateral onset to a large proportion,
(2) resting tremor,
(3) gradual slowing down of disease progression,
(4) limbs asymmetrically affected after the onset of PD, and
(5) treatment by levodopa featuring a certain effect.

HC: Volunteers diagnosed as healthy by clinical and imaging examinations were included, and those with neuropsychiatric disorders, intracranial infections, trauma, vascular and space-occupying lesions, and dysfunction of other organs were excluded.

2.3. Exclusion criteria

The exclusion criteria are as follows;

(1) history of apoplexia cerebri, brain injury, and encephalitis;
(2) use of antipsychotic drugs;
(3) organic lesion observed in the brain CT;
(4) lack of treatment effects for high-dose levodopa.

2.4. Preparation of ^{11}C-β-CFT and ^{18}F-FDG

$^{11}CO_2$ was generated by an accelerator and transported to a synthesizer. The transport time was about 1 min. $^{11}CO_2$ was then converted into ^{11}C-triflate-CH_3 online. Next, ^{11}C-triflate-CH_3 was passed into the newly prepared nor-β-CFT in acetone solution containing 1.0 mg precursor, followed by a labeling reaction at 30°C for 3 minutes. The reaction liquid was diluted with water for injection and injected to the Plus Short tC_{18} column for solid-phase extraction. Then, the tC_{18} column was eluted with 20 mL water, followed by elution with 2 mL ethanol and addition of 18 mL water for injection. Finally, the ^{11}C-β-CFT injection was obtained after passing through a 0.22 μm filter membrane.

^{18}F was generated by an accelerator and transported to a synthesizer. The ^{18}F ions were chelated with potassium ions via K2.2.2. Under anhydrous conditions, the mannose triflate precursor was added to be converted into β-D-glucose-2,3,4,6-tetraacetate. After hydrolysis in sodium hydroxide, the product was transferred to the purification column for solid-phase extraction. Then, the column was eluted with 14 mL water for injection, and ^{18}F-FDG injection was obtained by passing the sample through a 0.22 μm filter membrane. The quality control results were shown in Table 1.

2.5. PET/CT scan

Before the ^{11}C-CFT PET/CT imaging, the patients discontinued the drug intake for 2 days to avoid the potential effect of anti-PD drugs on the results. After intravenous injection of ^{11}C-CFT (185–370 MBq) for 1 hour, Discovery VCT64 PET/CT scanner (GE Healthcare, Milwaukee, WI) was used for CT imaging of the brain. Topogram is first used to determine the scanning range from the top of the head to the lower end of the cerebellum. The CT image acquisition parameters include the following: voltage, 120 KW; tube current, 300 mAs; collimation, 5.0 mm; layer thickness, 2.5 mm; 0.6 ms/rev; pitch, 1.25 mm. After attenuation correction of the CT data, 3DPET/CT mode scanning acquisition is performed in the same scanning range with CT. Brain cross-section, coronal plane, sagittal plane, and 3D reconstruction images of the subject are obtained by computer processing.

^{18}F-FDG PET/CT imaging was performed 2 days after the ^{11}C-CFT PET/CT imaging. All subjects were fasted for at least 8 hours before imaging. Any drugs that might influence the brain activity were discontinued for at least 12 hours before the ^{18}F-FDG PET/CT imaging. After ensuring that the blood glucose level was below 8 mmol/L, the intravenous injection of ^{18}F-FDG 3.7 MBq/kg was performed. The images were acquired 1 hour later in a quiet state, with the patients keeping their eyes closed. The configuration for image acquisition and data reconstruction was the same as that with the ^{11}C-CFT PET/CT imaging.

2.6. Analytical method of PET/CT images

2.6.1. ^{18}F-FDG imaging. The clearest cross-sectional images of the basal ganglia from CT are selected with the cerebellum as a reference. The brain's glucose metabolism function in this area is reflected by delineating the head of bilateral caudate nucleus, the bilateral putamen, and the surrounding brain parenchyma as the regions of interest (ROI) in ^{18}F-FDG imaging. Mean radioactivity counts in the ROI are calculated by obtaining the average for 3 layers and conducting the semi-quantitative analysis of the reduction area for cerebral cortex metabolism in several patients with PD.

2.6.2. ^{11}C-CFT imaging. The 3 clearest cross-sectional images of the basal ganglia from CT are selected with the cerebellum as a reference. The number and function of corresponding parts of DAT are semi-quantitative reflections of delineating the bilateral caudate nucleus, putamen, and encephalion (CB) as the ROI in the ^{11}C-CFT imaging. The semi-quantitative value of DAT distribution is obtained using the following formula: ^{11}C-CFT absorbing value = (ROI − CB)/CB.[14–15]

2.6.3. PET/CT image interpretation. ^{11}C-CFT and ^{18}F-FDG PET/CT images were retrospectively interpreted by the consensus of 2 experienced radiologists (Li Xiaohong and Qin Yongde with 10 and 30 years of experience in neurology PET, respectively) who had no knowledge of the other imaging results or the clinical data.

2.7. Statistical methods

SPSS 17.0 software is used for the statistical analysis. The semi-quantitative mean value of ^{11}C-CFT absorption in the bilateral basal ganglia between the PD and HC groups is compared by 2 independent samples t, which show significance at $P \leq .05$. The semi-quantitative mean value of ^{11}C-CFT absorption values is tested by 2 independent samples t, with $P \leq .05$ indicating statistical significance (the above measurement data are all expressed as $\bar{x} \pm s$).

3. Results

3.1. Clinical data of subjects in each group

As shown in Table 2. The 2 groups of subjects showed no significant difference in gender and age ($P > .05$).

3.2. ^{18}F-FDG PET/CT imaging results of PD group

According to semi-quantitative analysis, several patients with PD show an increased glucose metabolism in the bilateral basal

Table 1

Quality control results of ^{18}F-FGD and ^{11}C-CFT.

	^{11}C-β-CFT		^{18}F-FDG	
Items	Ch. P	Produce	Ch. P	Produce
Character	Colorless clear liquid	Colorless clear liquid	Colorless clear liquid	Colorless clear liquid
pH	5–8	6.2	5–8	6.5
Radiochemical purity	>95%	97.2	>90%	94.2
Bacterial endotoxin (EU)	<15	2.65	<15	4.53
Sterility test	No bacterial growth	No bacterial growth	No bacterial growth	No bacterial growth
Radioactive concentration (MBq/mL)	≥370	493.4	≥370	694.7

11C-CFT= 11C-labeled 2-β-carbomethoxy-3-β-(4-fluorophenyl) tropane, 18F-FDG = 18-Fluorine flurodeoxyglucose.

Table 2

Clinical data of subjects in each group.

Item	Healthy control		Parkinson group		*P*-value
	Male	Female	Male	Female	
Age	60.94±5.77	60.35±8.41	61.58±11.03	61.18±8.62	.554
Gender	18	32	38	64	.880

ganglia and decreased cerebral glucose metabolism in different regions of the cerebral cortex. The following symptoms are observed:

(1) The symmetric radioactivity distribution of bilateral basal ganglia is increased in96 cases (94.11%);
(2) asymmetric radioactivity of basal ganglia is reduced in 3 cases (2.94%);
(3) no evident abnormalities are detected in the bilateral basal ganglia in 3 cases (2.94%).

The ^{18}F-FDG PET/CT imaging as shown in Figure 1.

In addition, different degrees of cerebral cortical metabolism (no abnormal density changes in the above sites are shown in CT) are observed in 63 patients. Reduced parietal, temporal lobe, and frontal lobe metabolisms are identified in 38 (37.25%), 15 (14.70%), and 7 patients (6.86%), respectively. Lastly, decreased occipital lobe metabolism is noted in 3 patients (2.94%), as shown in Table 3.

3.3. ^{11}C-CFT PET/CT imaging results

^{11}C-CFT is specifically concentrated in the bilateral basal ganglia (caudal nucleus and putamen) of the subject, whereas the radiation distribution in the cortex, thalamus, and cerebellum is extremely low. According to the involvement of the basal nucleus of PD basal ganglia, the ^{11}C-CFT PET/CT image is interpreted as follows: the radioactivity distribution of the putamen is slightly reduced at the posterior part but is normalat the anterior and middle parts. The light and moderate severities show that the radioactivity distribution of the putamen is reduced at the posterior part, slightly decreased at the middle part, and normal at the head part. A moderate severity shows that the radioactivity distribution of the posterior nucleus is substantially reduced, whereas that of the putamen nucleus is normal. The medium and high severities indicate that the radioactivity distribution in the posterior nucleus is reduced to defect, whereas that of the anterior portion of the putamen is normal. A high severity shows that the radioactivity distribution in the anterior, middle, and posterior portions of the shell nucleus is reduced to defect.

PD severity is graded in accordance with the involvement of the putamen of the basal ganglia in patients with PD as shown in the ^{11}C-CFT PET/CT images. The^{11}C-CFT absorbing values are measured for each basal ganglion. The light, light-middle, middle, middle-severe, and severe PD groups are compared with the HC group. Statistically significant differences are found amongthe^{11}C-CFT absorbing values for the bilateral basal ganglia caudate nucleus and bilateral anterior, middle, and posterior putamen of each PD group and the HC group ($P<.05$). As shown in Figure 2.

^{11}C-CFT PET/CT images of HC group as shown in Figure 3A. Lightly severe unilateral basal ganglia are observed in 21 cases, in which the radioactivity distribution of the putamen is slightly reduced in the posterior part and is normal in the anterior and middle parts (Fig. 3B). The ^{11}C-CFT absorbing values of the caudate nucleus and the anterior, middle, and posterior parts of putamen in the HC group are reduced to 83.22%, 74.69%, 65.81%, and 66.43%, respectively.

Unilateral basal ganglia with light-moderate severity are observed in 18 cases, in which the radioactivity distribution of the putamen is reduced in the posterior part, slightly decreased in the middle part, and normal in the head part. The ^{11}C-CFT absorbing values of the caudate nucleus and the anterior, middle, and posterior parts of putamen in the HC group are reduced to 57.53%, 50.62%, 36.77%, and 27.97%, respectively.

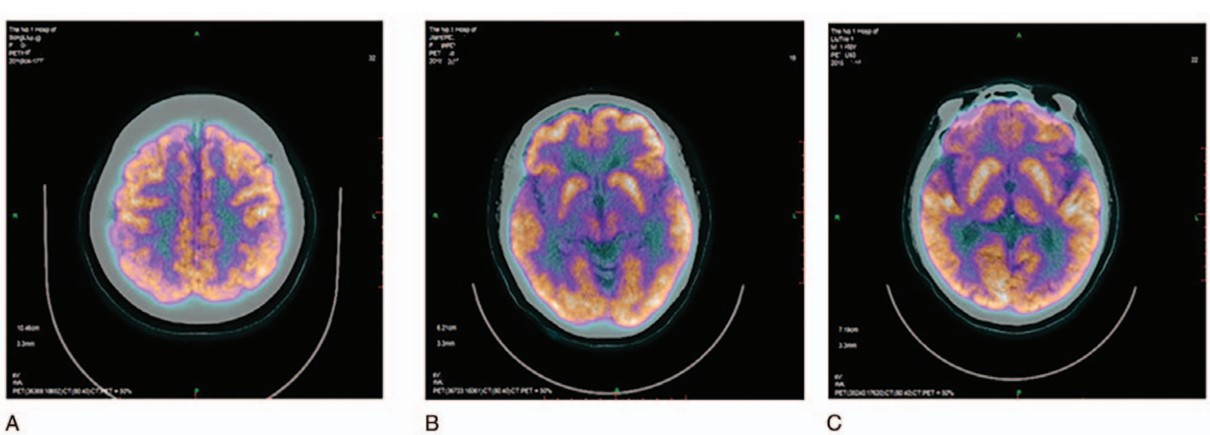

Figure 1. 18F-FDG PET/CT imaging (A): Reduced parietal metabolism in patients; (B): increased symmetric radioactivity distribution of bilateral basal ganglia; (C): reduced temporal lobe metabolism. 18F-FDG = 18-Fluorine flurodeoxyglucose, PET/CT = positron emission tomography/computed tomography.

Table 3

^{18}F-FDG uptake values in bilateral basal ganglia of each group.

Group		Light*		Middle*		Severe*	
		Uptake values	P	Uptake values	P	Uptake values	P
Right caudate nucleus	PD	1.14±0.21	.01	1.15±0.14	.00	1.18±0.09	.006
	HC	1.40±0.14		1.40±0.12		1.38±0.10	
Left caudate nucleus	PD	1.14±0.12	.01	1.15±0.10	.00	1.19±0.11	.024
	HC	1.40±0.07		1.40±0.09		1.40±0.07	
Right anterior putamen	PD	1.26±0.11	.147	1.27±0.17	.112	1.34±0.13	.451
	HC	1.45±0.17		1.47±0.14		1.51±0.18	
Left anterior putamen	PD	1.21±0.10	.001	1.31±0.14	.044	1.49±0.19	.874
	HC	1.47±0.18		1.49±0.17		1.52±0.17	
Middle part of right putamen	PD	1.39±0.07	.00	1.52±0.11	.00	1.56±0.06	.108
	HC	1.73±0.10		1.72±0.09		1.70±0.09	
Middle part of left putamen	PD	1.47±0.10	.001	1.46±0.14	.001	1.62±0.13	.334
	HC	1.73±0.04		1.70±0.10		1.71±0.11	
Posterior part of right putamen	PD	1.25±0.12	.041	1.38±0.13	.310	1.50±0.11	.871
	HC	1.45±0.17		1.48±0.11		1.53±0.14	
Posterior part of left putamen	PD	1.37±0.14	.154	1.27±0.11	.033	1.43±0.07	.457
	HC	1.49±0.13		1.48±0.17		1.49±0.12	

18F-FDG = 18-Fluorine flurodeoxyglucose.

* Grading according to ^{11}C-CFT imaging results.

Moderately severe unilateral basal ganglia are observed in 25 cases, in which the radioactivity distribution of the putamen is significantly reduced in the middle part and is normal in the anterior part (Fig. 3C). The ^{11}C-CFT absorbing values of the caudate nucleus and the anterior, middle, and posterior parts of putamen in the HC group are reduced to 59.59%, 49.38%, 33.87%, and 24.83%, respectively.

Moderately severe unilateral basal ganglia are observed in 22 cases, in which the radioactivity distribution of the putamen is significantly reduced to defect in the middle part and decreased in the anterior part. The ^{11}C-CFT absorbing values of the caudate nucleus and the anterior, middle, and posterior parts of putamen are reduced to 54.45%, 43.52%, 27.74%, and 22.38%, respectively.

Severe unilateral basal ganglia are observed in 16 cases, in which the radioactivity distribution of the putamen is sparsely reduced to defect in the middle part (Fig. 3D). The ^{11}C-CFT absorbing values of the caudate nucleus and the anterior, middle, and posterior parts of putamen are reduced to 40.41%, 31.48%, 21.29%, and 18.18%, respectively.

4. Discussion

PET/CT utilizes the anatomical advantages of CT images and reflects the physiological and metabolic characteristics of organs through localization and quantitative analysis. The combination of these techniques features notable potential and advantages. PET/CT imaging dynamically reflects the molecular-level information of PD brain glucose metabolism and DAT protein receptor. Its brain function imaging substantially influences the diagnosis and treatment guidance of neurological diseases. The characteristics of brain local metabolism, neurotransmitters, and receptors in vivo reflected by PET/CT imaging bear importance for the etiology and pathogenesis of related neurological encephalopathies, early and differential diagnoses, and objective evaluation of disease severity. This technique exhibits more quantitative analysis advantages than other imaging studies and has shown high clinical value.

Thinking and body movements are controlled by the brain's central region, the frontal lobe.[16] Bodily sensations are regulated by the parietal lobe region. Hearing, language, and memory are managed by the temporal lobe region. Integration of vision is governed by the occipital region.[17] Therefore, physical symptoms, such as decreased autonomic activity and slow movement of patients with PD, may be related to damages in these parts. A total of 102 patients with PD are analyzed in this study. Comparing the glucose metabolism in the brains of these patients with those of 50 HCs, 96 patients with PD exhibit bilateral metabolic changes in the basal ganglia as shown by ^{18}F-FDG PET/CT. Several patients also suffer from varying degrees of glucose metabolism in the frontal, parietal, temporal, and occipital regions of the brain. This finding is consistent with the previous domestic metabolic model of brain function in patients with PD.[18] Eidelberg[19] showed that the MSA patients differ significantly from the primary PD patients in terms of the PD-related pattern. In the former, the glucose metabolism decreased in the putamen and cerebellum, and the expression of the brain metabolic network was significantly lower than that of the latter. The PSP patients showed a reduced glucose metabolism in the brainstem and medial frontal lobe. The patients with CBD manifested a reduced glucose metabolism in the frontal, temporal, and parietal lobes on the affected side. The patients with Huntington disease exhibited a reduced in glucose metabolism in the caudate nucleus and putamen in the basal ganglia and in the medial temporal lobe of the cerebral cortex. By contrast, glucose hypermetabolism was detected in the occipital lobe. Thus, PD-related pattern could be used as basis for the differential diagnosis of PD. Atypical Parkinson syndrome and other dyskinesia disorders can be identified by PD glucose-related metabolic patterns.[20–21] Although brain glucose metabolism imaging shows the advantage of differential diagnosis, it cannot reflect the severity of the disease and presents certain limitations. Therefore, combining this method with ^{11}C-CFT brain DAT PET/CT imaging is necessary.

DAT imaging can assess the location, density, and function of DAT lesions and determine the severity of PD.[22–23] In PD

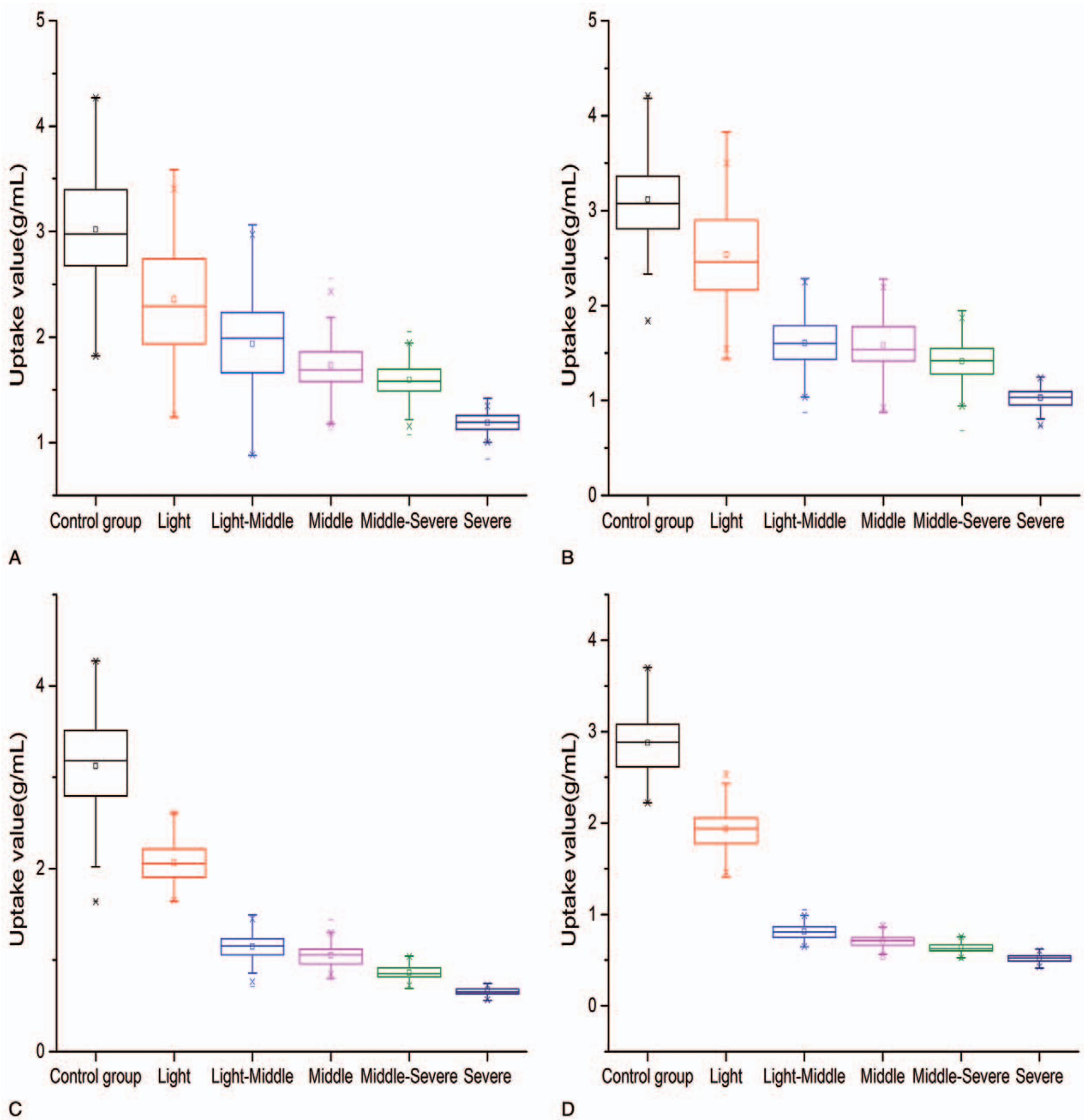

Figure 2. The uptake value of 11C-CFT PET (A): caudate nucleus; (B): anterior parts of putamen; (C): middle parts of putamen (D): posterior parts of putamen. 11C-CFT= 11C-labeled 2-β-carbomethoxy-3-β-(4-fluorophenyl) tropane, PET = positron emission tomography.

patients, given that the degeneration and attrition of the dopaminergic neurons in the substantia nigra are usually accompanied by a reduction in the amount and function of DAT on the presynaptic membrane, a reduced uptake of the contrast medium by the striatum indicates a decline in the DAT function. Studies[24–25] have noted the binding of ^{11}C-CFT to DAT with high specificity in the basal ganglia of PD patients. The^{11}C-CFT uptake in the basal ganglia of PD patients was significantly lower than that of the control group. The ^{11}C-CFT uptake was also significantly and negatively correlated to the H-Y staging and motor scores of Unified Parkinson Disease Rating Scale. Wang et al[24] showed an asymmetrical reduction in the ^{11}C-CFT uptake of bilateral putamina in the middle-stage PD patients, with the predominance of reduction in the contralateral side of the limb where the disease was initiated, especially in the posterior putamen. He et al[25] reported that during the ^{11}C-CFT PET imaging, the PD patients mainly presented with a significant reduction in radioactivity uptake in the bilateral caudate nuclei and putamina, especially in the medial and posterior putamina. The reduction was most pronounced in the bilateral caudate nuclei and putamina on the contralateral side of the affected limb. All the above studies show that ^{11}C-CFT PET imaging features a high sensitivity to detecting DAT changes in PD patients. With regard to the pathological process, ^{11}C-CFT PET/CT imaging of PD severity shows that the area of nucleus reduction is mainly affected by posterior involvement in patients with mild PD. In

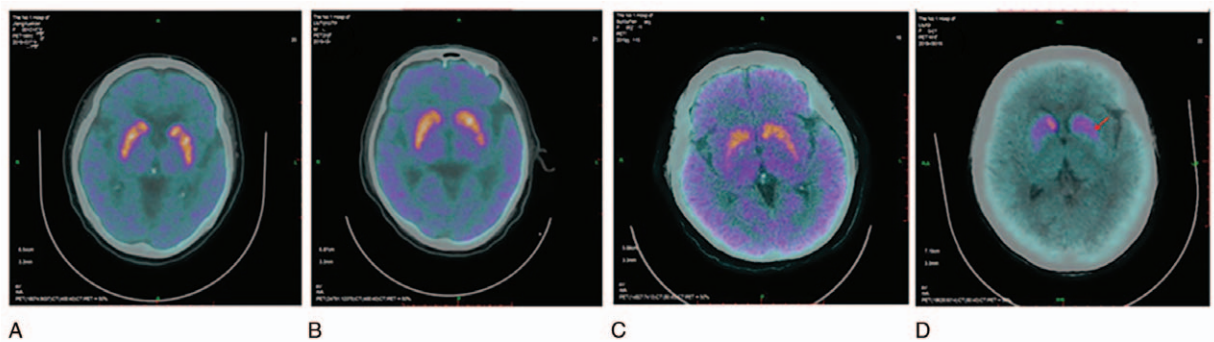

Figure 3. 11C-CFT PET/CT imaging (A): healthy control group, (B): slightly reduced radioactivity distribution of the putamen in the posterior part, (C): significantly reduced radioactivity distribution of the putamen in the middle part; (D): radioactivity distribution of the putamen sparsely reduced to defect in the middle part. 11C-CFT= 11C-labeled 2-β-carbomethoxy-3-β-(4-fluorophenyl) tropane, PET/CT = positron emission tomography/computed tomography.

patients with moderate PD, the main manifestation is the decreased ^{11}C-CFT absorption in the middle of the nucleus. The areas of nucleus reduction in patients with severe PD are mainly the anterior, middle, and posterior parts. When the condition of patients progresses, the ^{11}C-CFT absorbing value in the basal ganglia of the brain gradually accumulates in the anterior part of the putamen, whereas the amount in the posterior part of the nucleus reduces. The ^{11}C-CFT absorbing value of the basal ganglia of patients with PD decreases with the progress in diseases severity. Therefore, ^{11}C-CFT PET/CT imaging is a good indicator of PD diagnosis and severity. In the clinical diagnosis and treatment of PD, PET/CT should be combined with ^{18}F-FDG PET/CT and brain ^{11}C-CFT PET/CT imaging to further assist in the diagnosis and differential diagnosis. Combining these imaging methods could compensate for their shortcomings and fuse their respective advantages. Therefore, PET/CT dual imaging by ^{18}F-FDG brain metabolism combined with ^{11}C-CFT brain DAT features potential application value for the diagnosis and severity assessment of PD.

Altogether, DAT distribution features in ^{11}C-CFT PET/CT imaging can be combined with the semi-quantitative ^{11}C-CFT uptake and ^{18}F-FDG PET-CT imaging of the brain to achieve a better effect. The combined use of the 2 tracers cannot only improve the diagnosis of PD but also facilitate the severity evaluation of PD. However, our study faced certain limitations.

(1) DAT imaging may contain errors caused by variations in equipment, injection dose, and time.
(2) Thus far, no reference values are available for use as definite threshold values for PD severity grading.
(3) Whether ^{18}F-FDG PET imaging can be combined with ^{11}C-CFT PET imaging of the brain for efficient evaluation of PD patients after treatment remains to be further investigated.
(4) The application of combined imaging modalities is restricted due to the high irradiation dose and cost.

Author contributions

Data curation: Xiaohong Li, Qizhou Zhang, Yubin Li, Nazimuguli Mutaerbieke, Xiaojia Zhao, Amina Yibulayin.
Methodology: Qin Yongde.
Software: Qizhou Zhang, Yongde Qin.
Writing – original draft: Xiaohong Li, Qizhou Zhang.

References

[1] Aarsland D, Kurz MW. The epidemiology of dementia associated with Parkinson's disease. Brain Pathol 2010;20:633–9.
[2] Buchman AS, Shulman JM, Nag S, et al. Nigral pathology and parkinsonian signs in elders without Parkinson's disease. Ann Neurol 2012;71:258–66.
[3] Wang AQ, Kong LN, Meng MZ, et al. Mechanisms by which fibroblast growth factor 20 improves motor performance in a mouse model of Parkinson's disease. Neural Regen Res 2019;14:1438–44.
[4] Giovanni R, Massimiliano C, Simona A, et al. Accuracy of clinical diagnosis of Parkinson disease: a systematic review and meta-analysis. Neurology 2016;87:237–8.
[5] Charles HA, Thomas GB, Joseph GH, et al. Low clinical diagnostic accuracy of early vs advanced Parkinson disease. Neurology 2014; 83:406–12.
[6] Ling H, O'Sullivan SS, Holton JL, et al. Does corticobasal degeneration exist? A clinicopathological re-evaluation. Brain 2010;133:2045–57.
[7] Li YH, Wang SW, She YX, et al. The research of Parkinson's disease Patients'thalamus and striatum multimodal magnetic resonance imaging. J Clin Radiol 2018;37:1968–72.
[8] Gao Z, Wang W, Chen T, et al. Molecular imaging characteristics of dementia with Lewy bodies and Parkinson's disease with cognitive impairment (Chinese). Chin J Geriatr Heart Brain Vessel Dis 2017; 19:793–6.
[9] Pagano G, Yousaf T, Politis M. PET molecular imaging research of levodopa-induced dyskinesias in Parkinson's disease. Curr Neurol Neurosci 2017;17:90.
[10] Li WH, Lao-Kaim NP, Roussakis AA, et al. 11C-PE2I and 18F-Dopa PET for assessing progression rate in Parkinson's: a longitudinal study. Mov Disord 2017;33:117–27.
[11] Hughes AJ, Daniel SE, Kilford L, et al. Accuracy of clinical diagnosis of idiopathic Parkinson's disease: a clinico-pathological study of 100 cases. J Neurol Neurosurg Psychiatry 1992;55:181–4.
[12] Sanubaer M. Parkinson's Disease With Cerebrovascular Disesase Risk Factor Analysis (Chinese). Urumqi: Xinjaing Medical University; 2013.
[13] Li SJ. A Research of Current Perception Threshold of Median Nerve of Parkinson's Disease Patients Associated With Pain (Chinese). Suzhou: Soochow University; 2015.
[14] Wang J, Zuo CT, Jiang YP, et al. 18F-FP-CIT PET imaging and SPM analysis of dopamine transporters in Parkinson's disease in various Hoehn & Yahr stages. J Neurol 2007;254:185–90.
[15] Lin W, Wu JJ, Guo SS, et al. Dopamine transporter PET imaging in patients with freezing of gait of Parkinson's disease (Chinese). Chin J Clin Neurosci 2015;23:268–73.
[16] Yang X. The Study of Brain-Computer Interface Based on Animal Experiments (Chinese). Hang zhou: Zhejiang University; 2007.
[17] Zhao YL. An Functional MRI Study of Sensation and Sensorimotor Integration Deficits in Early Parkinson's Disease (Chinese). Hang Zhou: Zhejiang University; 2009.
[18] Shi XC, Chen L, Zhang XS, et al. Brain glucose metabolism in Parkinson's disease (Chinese). Chin J Nerv Ment Dis 2011;37:565–8.

[19] Eidelberg D. Metabolic brain networks in neurodegenerative disorders: a functional imaging approach. Trends Nanrosci 2009;32:548–57.
[20] Matthews DC, Lerman H, Lukic A, et al. FDG PET Parkinson's disease-related pattern as a biomarker for clinical trials in early stage disease. Neuroimage Clin 2018;20:572–9.
[21] Tomše P, Jensterle L, Rep S, et al. The effect of 18F-FDG-PET image reconstruction algorithms on the expression of characteristic metabolic brain network in Parkinson's disease. Phys Med 2017;41:129–35.
[22] Chung SJ, Yoo HS, Lee YH, et al. Heterogeneous patterns of striatal dopamine loss in patients with young- versus old-onset Parkinson's disease: impact on clinical features. J Mov Disord 2019;12:113–9.
[23] Fu JF, Klyuzhin I, McKenzie J, et al. Joint pattern analysis applied to PET DAT and VMAT2 imaging reveals new insights into Parkinson's disease induced presynaptic alterations. Neuroimage Clin 2019;23:101856.
[24] Wang HC, Zuo CT, Huang ZM, et al. Application of 11C-CFT PET in the diagnosis of Parkinson's disease with early-stage. J China Clinic Med Imaging 2010;21:229–32.
[25] He TT, Wang RM, Chen YM, et al. PET imaging of dopamine transporter (DAT) in the diagnosis of Parkinson's disease. Chin J Med Imaging 2008;16:94–7.